2010-01-0166

Ethanol Content Estimation in Flex Fuel Direct Injection Engines Using In-Cylinder Pressure Measurements

Kyung-ho Ahn and Anna Stefanopoulou
University of Michigan

Li Jiang and Hakan Yilmaz
Robert Bosch LLC

ABSTRACT

Flexible fuel vehicles (FFVs) are able to operate on a blend of ethanol and gasoline in any volumetric concentration of up to 85% ethanol (93% in Brazil). The estimation of ethanol content is crucial for optimized and robust performance in such vehicles. Even if an ethanol sensor is utilized, an estimation scheme independent of the ethanol sensor measurement retains advantages in enhancing the reliability of ethanol estimation and allowing on-board diagnostics. It is well-known that an exhaust gas oxygen (EGO) sensor could be utilized to estimate the ethanol content, which exploits the difference in stoichiometric air-to-fuel ratio (SAFR) between ethanol (9.0) and gasoline (14.6). The SAFR-based ethanol estimation has been shown to be prone to large errors with mass air flow sensor bias and/or fuel injector shift. In this paper, an ethanol estimation scheme is proposed by additionally using measurement of in-cylinder pressure, which essentially exploits the difference in latent heat of vaporization (LHV) between ethanol and gasoline, and hence detects the charge cooling effects of ethanol. Due to the additional and independent information introduced by the new algorithm, the proposed ethanol content estimation is more tolerant to air flow sensor drifts and injector shifts.

1 INTRODUCTION

Flexible fuel vehicles can operate on a blend of gasoline and ethanol in any concentration of up to 85% ethanol. This blend is denoted by the EXX nomenclature, where XX represents the volumetric percentage of ethanol in the gasoline-ethanol blend. E85 is a commercially available fuel in the United States.

Ethanol and gasoline have different physical properties as shown in Table 1 [1, 2] which affect vehicle performance and FFVs need to adapt, and ideally, optimize the engine calibration depending on the estimated fuel ethanol content. The estimation of ethanol content in the fuel relies on the differences in the fuel properties between ethanol and gasoline. The drastic difference in the dielectric constant between gasoline and ethanol (Table 1) enables capacitance-based sensing of the ethanol content in the fuel [3]. Apart from the cost and reliability issues associated with such sensors, on-board diagnostic (OBD) requirements would necessitate an additional method for assessing the ethanol content in order to diagnose any faults or degradation in sensors associated with the ethanol estimation.

Table 1: Properties of gasoline and ethanol

Property	Gasoline	Ethanol
Research Octane Number (RON)	92	111
Density (kg/m^3)	747	789
Heat of combustion (MJ/kg)	42.4	26.8
Stoichiometric air-to-fuel ratio	14.6	9.0
Boiling point (°C)	20-300	78.5
Latent heat of vaporization (kJ/kg)	420	845
Dielectric constant	2.0	24.3

Independent ethanol content estimation can be based on the other properties of Table 1. Each physical property in the table is defined as a *primitive feature* in this paper. If a primitive feature could be directly measured, the fuel ethanol content can be calculated from the feature. A high sensitivity of the feature to the ethanol content is desirable, as a higher sensitivity results in higher estimation accuracy or confidence. In this sense, apart from the dielectric constant, the stoichiometric AFR (SAFR), the latent heat of vaporization (LHV), the heat of combustion (HC), and the RON are very good primitive features for

estimation of fuel ethanol content.

Among the primitive features, stoichiometric air-to-fuel ratio (SAFR) is the feature which can be indirectly calculated using an EGO sensor given the amount of cylinder air charge and injected fuel. Since an EGO sensor is inevitably used for closed-loop regulation of the air-to-fuel ratio, utilizing an EGO sensor is the simplest and the most popular way of ethanol content estimation. The main disadvantage of SAFR-based ethanol estimation is the high sensitivity of ethanol content estimation to mass air flow (MAF) sensor drift and/or fuel injector shift [4, 5]. Note here that the current practice of estimating MAF drifts and switching to ethanol content estimation immediately after refueling is prone to error accumulation [6]. In [6] we proposed a seamless way for estimating simultaneously MAF sensor drifts and ethanol content changes by combining measurements from the intake manifold pressure (manifold absolute pressure, MAP) sensor.

We propose here, an even more complete sensor fusion which enables simultaneous estimation of ethanol content, MAF sensor drifts and fuel injector shifts. The proposed scheme utilizes the LHV feature of ethanol detection from Table 1. Specifically, it fuses information on charge cooling due to LHV of ethanol via cylinder pressure, hence it can only be applied to direct injection engines with in-cylinder pressure sensor.

Ethanol detection residue which is derived from the primitive feature of LHV by using in-cylinder pressure measurements during the compression stroke in a direct injection (DI) engine was proposed and analyzed in [7] as a candidate feature to estimate fuel ethanol content from. The LHV-based detection residue was shown to be a good feature due to the observed monotonic behavior of the residue with respect to change of ethanol content at several commonly visited operating conditions. Since in-cylinder pressure measurements are considered in many advanced engines for closed loop control of combustion, ethanol estimation and fuel diagnostics could be an additional advantage in engines with such in-cylinder pressure measurements.

Note here that heat of combustion (HC) is another good primitive feature from Table 1 but shows very similar sensitivity to that of SAFR: HC shows -37% change from gasoline to ethanol and 58% change from ethanol to gasoline, and SAFR shows -38% change from gasoline to ethanol and 59% change from ethanol to gasoline. Therefore, we expect, to some extent, that HC-based ethanol estimation might overlap with the SAFR-based method providing redundant but not independent information regarding ethanol content. More comprehensive discussion of redundancy is provided in the appendix. Accordingly, a question arises whether the LHV-based detection residue could be independently utilized in ethanol estimation of the SAFR-based approach or it also overlaps with the SAFR-based scheme reducing the value of using an independent feature with respect to λ[1]. In this paper, it will be demonstrated that the LHV-based ethanol detection residue could actually serve as an independent feature of λ in ethanol estimation.

Specifically, a data-driven LHV-based ethanol detection model is presented in this paper to demonstrate ethanol content estimation. Using this LHV-based estimation, together with the SAFR-based approach, a composite ethanol content estimation scheme will be proposed and its validity will be demonstrated by a realistic simulation. Apart from developing an ethanol estimation scheme that is tolerant to air flow sensor drifts and injector shifts, the algorithm explicitly calculates the sensor drift and injector shift, hence can be used for fuel injection diagnostics purposes in addition to ethanol detection.

2 LHV-BASED ETHANOL DETECTION RESIDUE

A detection feature calculated by in-cylinder pressure measurements and motivated by the different latent heat of vaporization between gasoline and ethanol is proposed in [7, 8]. After fuel is injected into the cylinder during closed valves, the injected fuel takes heat from the cylinder charge while it is vaporizing, hence causing a charge cooling. The charge cooling effect may be observable in cylinder pressure measurement, where more charge cooling or less cylinder pressure is expected for higher LHV or higher ethanol content. To differentiate the charge cooling effect from the other thermo-physical phenomena and their effects on cylinder pressure evolution, we compare the cylinder pressures from two different injection modes while keeping all other inputs fixed.

- Single injection (Si) mode: all the fuel is injected during the intake stroke, hence the charge cooling observed by cylinder pressure should be minimal.
- Split injection (Sp) mode: a fraction of the fuel is injected during the intake stroke, and the rest is injected during compression stroke after intake valve is closed. The second portion of the fuel that is injected during the compression stroke is responsible for in-cylinder charge cooling, and an associated pressure drop could be observed. The observed pressure drop (as shown in the first subplot of Fig. 1) is associated with the heat of vaporization, and consequently the ethanol content.

The ethanol detection residue at an instance is calculated as:

$$Rsd(k) = \ln(p_0^{Si}(k)/p_0^{Sp}(k)), \quad (1)$$

where p_0^{Si}, p_0^{Sp} are corrected cylinder pressures [7] under Si and Sp injection modes, and k denotes a step in time or crank angle. Even though the cylinder pressures under different modes are obtained in different cycles, we regard

[1] The relative air-to-fuel ratio (AFR), λ, is defined as the ratio of actual AFR (AFR) to stoichiometric AFR (AFR_s), i.e., $\lambda \triangleq AFR/AFR_s$.

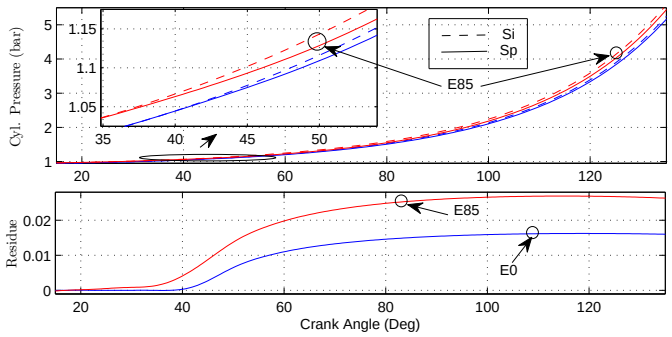

Figure 1: Cylinder pressure and residue evolutions during the compression stroke

them as synchronized quantities in time. Fig. 1 demonstrates the general evolution of the residue (1) during the compression stroke. To utilize the detection residue as a detection feature, the mean residue is calculated by averaging Rsd over the interval of several steps near the end of compression where the instantaneous residue is usually maximized:

$$r_{LHV} = \frac{\sum_{k=k_1}^{k_2} Rsd(k)}{k_2 - k_1 + 1}. \tag{2}$$

3 STOICHIOMETRIC BI-AFFINE RESIDUE MODEL

We model the mean residue (2) as a simple polynomial map parameterized by several operating condition variables and identify the coefficients in the polynomial from experimental residue data. When we model, identify and validate a detection feature function, we are actually interested in the detection feature function restricted at stoichiometry because stoichiometry is a normal operating condition enforced by closed-loop control. For the same reason, we usually collect experimental measurement data only at stoichiometry to validate a detection feature model. Therefore, we frequently know r_s rather than r, where r_s denotes restriction of detection feature r at stoichiometry, i.e., $r_s = r\big|_{m_a/m_f = AFR_s(e)}$, where m_a and m_f denotes fresh air mass trapped in the cylinder and fuel mass injected into the cylinder per cycle, respectively, and $AFR_s(e)$ denotes the stoichiometric air-to-fuel ratio evaluated at the volumetric fraction of ethanol in the fuel blend e. Fig. 2 illustrates a detection feature at fixed ethanol content and any other operating condition variables, $\boldsymbol{q}$, other than m_f and m_a. Among the candidate data on detection feature surface, we usually collect data along the stoichiometric detection feature curve in the figure. Therefore, the stoichiometric residue model r_s will be parameterized by injected fuel mass m_f, but not by air charge m_a. For brevity, we will call the mean residue simply residue and drop operating condition notation $\boldsymbol{q}$ which denotes any other operating condition variables than e and m_f such as engine speed N, valve timing and so on, which are held at fixed conditions. Some of those conditions will be specified if clarification is necessary. In a fixed operating condition $\boldsymbol{q}$, we use a stoichiometric residue model which

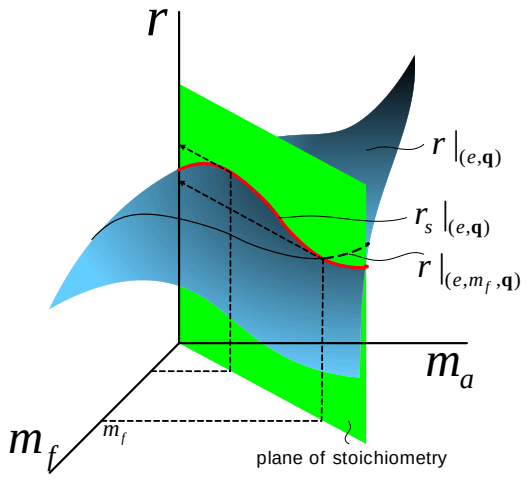

Figure 2: A detection feature and its restriction at stoichiometry demonstrated at fixed $(e, \boldsymbol{q})$

is expressed by a bi-affine function in e and m_f:

$$r_s = a_1 + a_2 m_f + a_3 e + a_4 m_f e. \tag{3}$$

In order to identify the coefficients in the model (3), we have used experimental data collected at near-stoichiometry on a 2.0L Turbocharged spark ignition direct injection (SIDI) variable valve timing (VVT) engine equipped with Kistler 6125B in-cylinder pressure sensors. Table 2 summarizes the nominal conditions for the experiments.

Table 2: Nominal experiment conditions

Description	Value
Relative AFR (λ)	1
Split injection ratio (Sp mode)	50/50 (%)
Start of 1st injection	105 CAdeg bBDC
End of 2nd injection (Sp mode)	40 CAdeg aBDC
Spark timing	MBT map for E0

Fig. 3 shows an example of the computed residue at two engine speeds 2000 and 2500 RPM and several air flows. The data were collected at several air flows and speeds utilizing the VVT and spark timing settings associated with the E0 calibration of the given speeds and loads. As the data indicates there was a small variability between the nominal and the actual mass air flow since not all the data are lined-up vertically. There is also considerable cycle-to-cycle variability observed in the data. Each data point corresponds to a couple of cycles, since the residue is extracted by comparing one cycle for Si injection mode and the other for Sp injection mode. The total number of data points for each nominally set MAF value is over 390. The circles correspond to the regression model (3) derived by considering all the data using standard least squares method. In the plots shown by error bars, the middle point of an error bar corresponds to the average

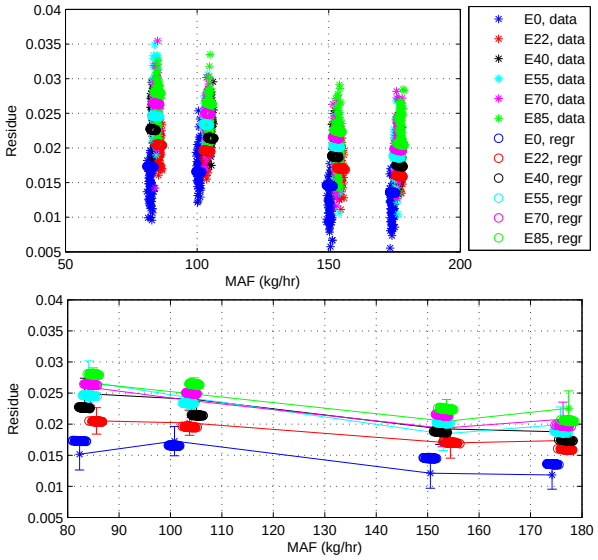

(a) Engine speed of 2000 RPM

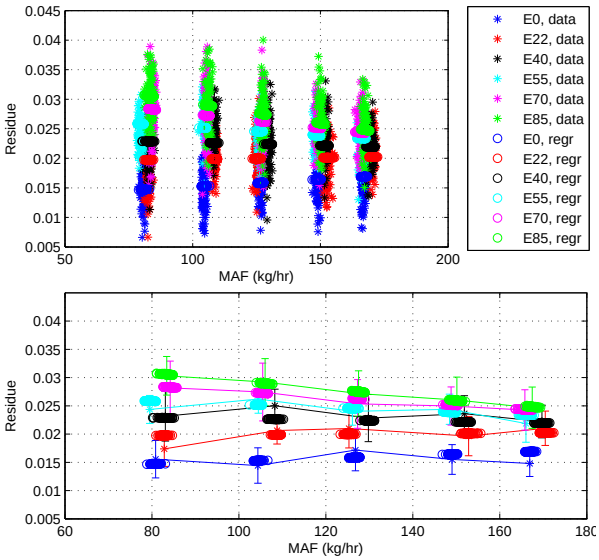

(b) Engine speed of 2500 RPM

Figure 3: Stoichiometric residue regression

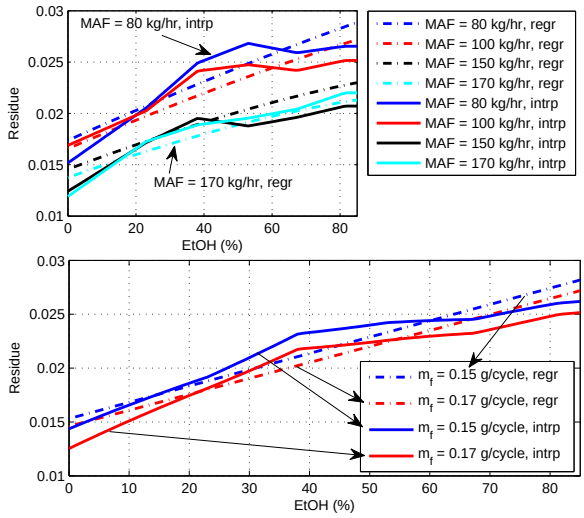

(a) Engine speed of 2000 RPM

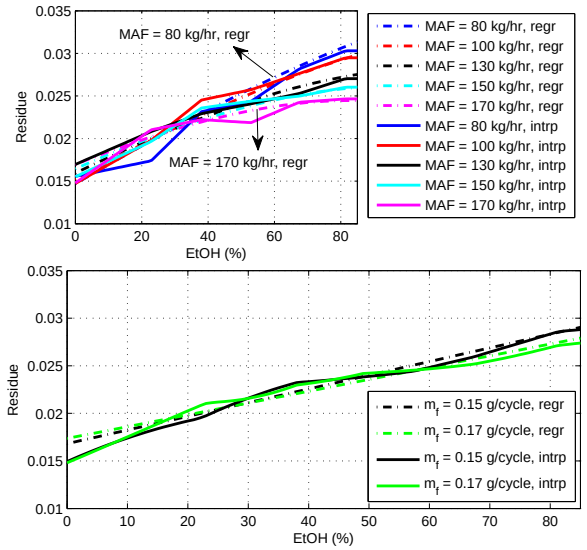

(b) Engine speed of 2500 RPM

Figure 4: Stoichiometric bi-affine residue model

residue for one fuel blend at a nominal MAF, and the error bar indicates the standard deviation. Due to the high cycle-to-cycle variability of combustion and pressure evolution, hence residue, the root mean square error is actually high: normalized root mean square errors (NRMSE) are 0.101 and 0.108 for 2000 RPM and 2500 RPM, respectively. Therefore, a filter with low cut-off frequency or a low gain observer or a large averaging window is necessary in on-line estimation to cope with the residue cycle-to-cycle variability, hence expecting slow ethanol estimation to some extent.

Fig. 4 shows the residue in a more interesting perspective. Given constant air flow, or equivalently, fuel flow the plot of the residue versus ethanol content shows a clear trend where residue increases when ethanol content increases. The dash-dot lines in Fig. 4 show the modeled stoichiometric residue using regression (3) versus fuel ethanol content at several MAF conditions of stoichiometry and at two different injected fuel mass conditions of stoichiometry. The solid lines correspond to the interpolated residue obtained by averaging data at the same nominal conditions and interpolating the averaged residues as discussed in Fig. 3. The solid lines in Fig. 4 could be realized in a micro-controller with a stored look-up table, whereas the dash-dot lines could be realized by programming (3) in the on-board micro-controller. We distinguish between these two implementations due to their differences around the 30-50% ethanol concentration and their implications to the estimation feasibility and accuracy. The data and hence the interpolation method exhibit a non-monotonic, strong non-linear behavior at 30-50% ethanol concentration due to the underlying physics regarding the nonlinear characteristics of vapor pressure of the gasoline-ethanol blend. Mixing a small amount of a gasoline-ethanol blend with a large amount of gasoline can produce a mixture with a higher vapor pressure than either the gasoline or the blend alone [9, 10, 11]. Nonlinear vapor pressure to

ethanol concentration, hence the non-ideal solution behavior of gasoline-ethanol blend may result in nonlinear behavior of the residue.

4 STEADY STATE ANALYSIS OF ETHANOL ESTIMATION UNDER FUEL INJECTOR SHIFT

In this section, the steady state analysis of LHV-based estimation under fuel injector shift will be provided. To compare the analysis with the SAFR-based estimation, the steady state analysis of SAFR-based estimation using the λ model, $\lambda = \frac{m_a}{m_f} \cdot \frac{1}{AFR_s(e)}$, is first reviewed.

4.1 SAFR-BASED ESTIMATION

Assuming no fault in EGO sensor, let us introduce MAF sensor error so that $\hat{m}_a = (1 + f_{ea})m_a$, where $\hat{m}_a$ denotes the estimated cylinder air charge mass, m_a the actual air charge and f_{ea} the air mass error fraction. Together with the fuel injector shift, where f_{ef} denotes the fuel injector shift such that $m_f = (1 + f_{ef})m_{inj}$, where m_{inj} is commanded or issued amount of fuel and m_f is the actual fuel amount injected into the cylinder, the actual AFR is the same as the stoichiometric AFR at stoichiometry, $m_a/m_f = AFR_s$, hence resulting in:

$$AFR_s = \frac{1}{(1 + f_{ea})(1 + f_{ef})} \frac{\hat{m}_a}{m_{inj}}. \quad (4)$$

In steady state, the fuel injection command is solely determined by the feedforward command based on the assumed or estimated stoichiometric AFR by $m_{inj} = \hat{m}_a/\widehat{AFR}_s$. Equation (4) is then expressed by:

$$\frac{\widehat{AFR}_s}{AFR_s} = (1 + f_{ea})(1 + f_{ef}). \quad (5)$$

Equation (5) describes how the MAF sensor error and fuel injection error propagate to error in estimation of stoichiometric AFR. The stoichiometric AFR for ethanol-gasoline mixture is expressed by $AFR_s = 9 \times e_m + 14.6 \times (1 - e_m) = 14.6 - 5.6 \times e_m$, where e_m denotes mass fraction of ethanol in the fuel blend. From (5), the following steady state mass ethanol fraction estimation result using SAFR-based estimation is then obtained:

$$\hat{e}_{m,ss,SAFR}(e_m, f_{ef}, f_{ea}) = e_m - f_e(f_{ef}, f_{ea})(2.6 - e_m), \quad (6)$$

where $f_e(f_{ef}, f_{ea}) = f_{ef} + f_{ea} + f_{ef} f_{ea}$.

4.2 LHV-BASED ESTIMATION

In the steady state analysis of LHV-based estimation under stoichiometric conditions, we distinguish regressed residue, $r_s^{regr}(m_f, e) = a_1 + a_2 m_f + a_3 e + a_4 m_f e$, from interpolated residue $r_s^{intrp}(m_f, e)$ corresponding to the interpolated data curves in Fig. 4. The actual residues assuming fuel injector shift f_{ef} are then expressed by $r_{s,act}^{regr}(m_{inj}, e, f_{ef}) = r_s^{regr}((1 + f_{ef})m_{inj}, e)$ and $r_{s,act}^{intrp}(m_{inj}, e, f_{ef}) = r_s^{intrp}((1 + f_{ef})m_{inj}, e)$. By inverting the residue function (3) with respect to e at $m_f = m_{inj}$, the steady state volumetric ethanol fraction estimations are obtained:

$$\hat{e}_{ss,LHV}^{regr} = \frac{r_s^{regr}((1 + f_{ef})m_{inj}, e) - a_1 - a_2 m_{inj}}{a_3 + a_4 m_{inj}}, \quad (7)$$

$$\hat{e}_{ss,LHV}^{intrp} = \frac{r_s^{intrp}((1 + f_{ef})m_{inj}, e) - a_1 - a_2 m_{inj}}{a_3 + a_4 m_{inj}}. \quad (8)$$

The steady state estimation using the regressed actual residue is finally expressed as:

$$\hat{e}_{ss,LHV}^{regr}(e, f_{ef}, m_{inj}) = e + f_{ef} \cdot m_{inj} \cdot \frac{a_2 + a_4 e}{a_3 + a_4 m_{inj}}. \quad (9)$$

Fig. 5 shows steady state ethanol estimation using the stoichiometric bi-affine residue model from (3) at engine rotation speed of 2000 RPM and 100 kg/hr MAF, and engine rotation speed of 2500 RPM and 130 kg/hr MAF, compared with the SAFR-based estimation with no MAF sensor error. Overall, the LHV-based estimation is less sensitive to fuel injection shift when compared with SAFR-based estimation. Especially low sensitivity is observed around 30% ethanol content at 2500 RPM. Although the estimation result with regressed actual residue ($\hat{e}_{ss,LHV}^{regr}$) is very good at every condition, the ethanol content estimation with interpolated actual residue ($\hat{e}_{ss,LHV}^{intrp}$) is very poor for 2000 RPM around 40% to 80% ethanol contents where the interpolated residue had highly non-linear and non-monotonic behavior.

5 FEASIBILITY OF COMPOSITE ESTIMATION

Here we show that LHV-based estimation is a truly independent ethanol estimation scheme of SAFR-based estimation, which actually means it can provide independent and valuable information for the ethanol estimation. If LHV-based estimation is an independent scheme of SAFR-based estimation, the injector shift f_{ef}, or equivalently, the actual fuel amount m_f, and the ethanol content e, should be able to be simultaneously solved by imposing the stoichiometric condition $m_a/m_f = AFR_s(e)$ to the following measurement equations associated with λ and LHV-based residue r_{LHV}:

$$\lambda = \frac{m_a}{m_f} \cdot \frac{1}{AFR_s(e)}, \quad (10)$$

$$r_{LHV} = r_{LHV}(m_a, m_f, e). \quad (11)$$

By the stoichiometry constraint, (10) trivially reduces to $\lambda = 1$ and (11) to the stoichiometric residue equation, $r_{LHV} = r_s(m_f, e)$ whose bi-affine parameterized model is (3), or,

$$r_{LHV} = r_s(m_a/AFR_s(e), e). \quad (12)$$

Let $r_s^a(m_a, e)$ denote the stoichiometric residue function parameterized by m_a and e, i.e., $r_s^a(m_a, e) = r_s(m_a/AFR_s(e), e)$. The residue measurement equation (12) is then expressed as:

$$r_{LHV} = r_s^a(m_a, e). \quad (13)$$

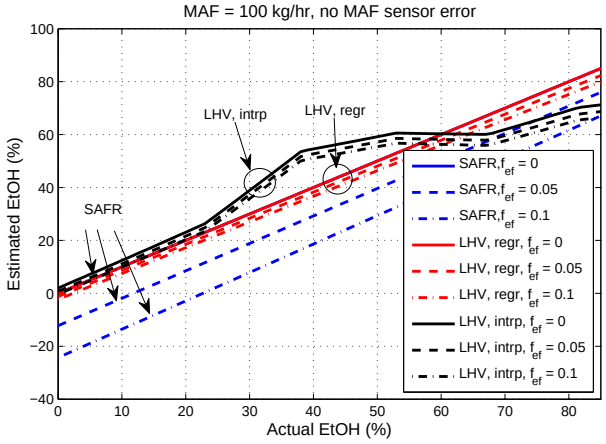

(a) Engine speed of 2000 RPM

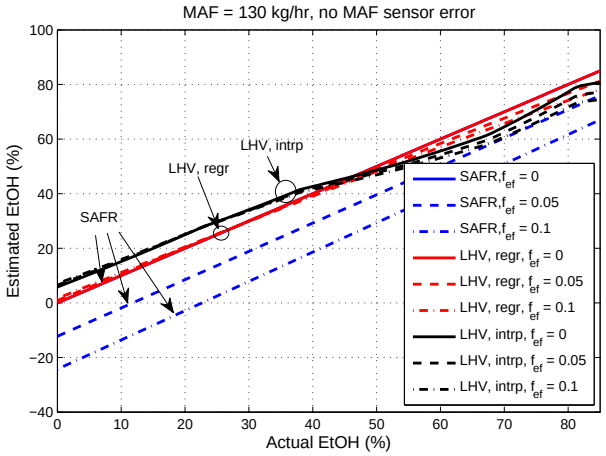

(b) Engine speed of 2500 RPM

Figure 5: Steady state ethanol estimation using LHV-based estimation compared with SAFR-based estimation

To solve unknown e from (13), r_s^a should be invertible at known air mass m_a. The curves in the first plots of each subplot in Fig. 4 correspond to the function r_s^a at several known air masses. Based on the regression curves, r_s^a is invertible at known air mass m_a, hence e can be solved. As several interpolated curves are not monotonic, the independence argument is only based on the regression models in more strict sense. The invertibility of r_s^a at fixed air mass, or equivalently independence of two different estimation schemes, relies on the monotonicity of the residue, and high sensitivity of the residue to ethanol content at fixed air mass is desirable. The fuel amount is then solved by $m_f = m_a/AFR_s(e)$.

The independence of two different schemes is also clear from the steady state ethanol content estimations (6) and (9) under different estimation schemes. Independence of the two schemes would result in different mappings of the steady state estimations from e and f_{ef}. In Fig. 5, both ethanol content estimations show the sensitivities to the actual ethanol content always around 1, i.e., the slopes of curves are almost unity, while the SAFR-based estimation is more sensitive to the fuel injection shift than the LHV-based estimation.

6 COMPOSITE ETHANOL ESTIMATION

Even though the detection residue model has large errors in some operating conditions, as at 2000 RPM, the residue model could be utilized for composite estimation together with EGO sensor measurements in some limited operating conditions to simultaneously estimate the ethanol content and the fuel injector shift. The ethanol estimation performance might be enhanced compared with the SAFR-based scheme under fuel injector shift by augmenting the LHV-based scheme with the SAFR-based method.

Fig. 6 shows a block diagram of AFR control and composite ethanol estimation in a flex fuel vehicle equipped with a direct injection engine. In the engine block, air flow is generally measured at a block located before the intake manifold, denoted by $\overline{W}_a$. We assume that the air flow measurement has bias so that $\overline{W}_a = (1+f_{ea})W_a$ in steady state, where f_{ea} denotes the error fraction in mass air flow measurement and W_a denotes the actual air flow at the measurement location. Accordingly, MAF measurement is expressed as $\overline{W}_a = (1+f_{ea})W_{cyl}$ in steady state, where W_{cyl} denotes the actual air flow inducted into the cylinder. Cylinder flow estimator estimates W_{cyl} while updating the bias estimation $\hat{f}_{ea}$ inside the block using various measurements such as engine rotation speed, intake manifold pressure and temperature, exhaust manifold pressure and temperature, if any are required for robust estimation of W_{cyl}. This estimation block could be generally realized by adapting the algorithm in [6] to different pumping maps whose inputs are different for different engine configurations.

In the cylinder block, we assume that the actual fuel flow into the cylinder is expressed by $W_f = (1 + f_{ef})W_{inj}$ by the fuel injector shift, where W_{inj} denotes the fuel flow commanded to the fuel injector and f_{ef} denotes the error fraction in the injection amount by the fuel injector shift.

The AFR controller is expressed as:

$$W_{inj} = W_{ff} + W_{fb}, \tag{14}$$

$$W_{ff} = \frac{\widehat{W}_{cyl}}{\widehat{AFR}_s} \cdot \frac{1}{1+\hat{f}_{ef}}, \tag{15}$$

$$W_{fb} = -C_{fb}(s)(1-\lambda), \quad C_{fb}(s) = k_{PI}\frac{\tau_{PI}s+1}{s}, \tag{16}$$

where W_{ff} and W_{fb} denote the feedforward injection command and the feedback injection command, respectively, $\widehat{W}_{cyl}$ denotes the estimation of W_{cyl}, where the MAF sensor bias is corrected, $\widehat{AFR}_s$ denotes the estimated stoichiometric AFR calculated by the estimated ethanol content $\hat{e}$, $\hat{f}_{ef}$ denotes the estimation of f_{ef}, and k_{PI} and τ_{PI} are the proportional-integral (PI) feedback AFR control gains.

The composite ethanol content estimator which is able to simultaneously estimate the ethanol content, e, and the

fuel injector shift, f_{ef}, is designed to be:

$$\begin{bmatrix} \dot{\hat{e}} \\ \dot{\hat{f}}_{ef} \end{bmatrix} = \boldsymbol{L} \begin{bmatrix} W_{fb} \\ r_{LHV} - \hat{r}_s \end{bmatrix}, \tag{17}$$

where $\boldsymbol{L} \in \Re^{2\times 2}$ is an observer (or filter) gain, r_{LHV} is the detection residue calculated by using the cylinder pressure measurements via (1)-(2), and $\hat{r}_s$ is the estimated stoichiometric residue calculated by $\hat{r}_s = r_s^{regr}(\hat{m}_f, \hat{e}) = a_1 + a_2\hat{m}_f + a_3\hat{e} + a_4\hat{m}_f\hat{e}$, where $\hat{m}_f$ is the estimated fuel injection mass per cycle calculated by $\hat{m}_f = (1+\hat{f}_{ef})m_{inj}$.

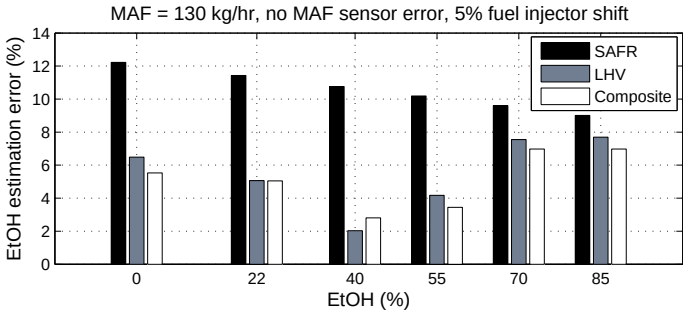

Figure 7: Steady state ethanol estimation error at engine speed of 2500 RPM under different estimation schemes

Fig. 7 shows steady state ethanol estimation errors at 130 kg/hr MAF and 2500 RPM engine speed assuming perfect air charge estimation, no MAF sensor error and 5% fuel injector shift. In the calculation, the real experimental residue data were used. The estimation errors under composite estimation scheme are compared with those under single-sensor-based schemes that use EGO sensor measurements and residue (in-cylinder pressure) measurements, respectively. The steady state estimation values were calculated by (6) for SAFR-based estimation and by (8) for LHV-based estimation, respectively. Likewise, steady state estimation under composite estimation is obtained by imposing equilibrium condition in the closed-loop system, i.e., solving $\frac{\widehat{AFR}_s}{AFR_s} = (1 + f_{ea})\frac{1+f_{ef}}{1+\hat{f}_{ef}}$ and $r_{LHV} = \hat{r}_s$ simultaneously. Note that the LHV-based estimation does not benefit in a significant way, when it is integrated with the SAFR-based estimation, forming the composite estimation. Indeed, the LHV-based estimation is insensitive and hence tolerant to fuel drift as originally indicated in section 4 Fig. 5. One can see that the composite scheme can hurt the LHV-based estimation when the SAFR-based estimation is very wrong as in 40% ethanol content in Fig. 7.

7 SIMULATION

So far we show the various estimation schemes of steady-state, but on-board implementation requires special attention to the non-steady conditions and noisy measurements. This section basically explores the transient issues of the composite estimation. Moreover, this section shows that using the dynamic inversion from (17) filters effectively the cycle-to-cycle variability associated with the residue calculations in (1)-(2) through the cylinder pressure measurements. In order to validate the composite ethanol estimation together with stoichiometry control, simulations were performed under ethanol content change in fuel blend and a throttle step change using the turbocharged SIDI VVT engine model in [12] for the engine block in Fig. 6. Engine rotation speed was fixed at 2500 RPM. Due to the lack of model for the detection residue r which covers off-stoichiometry condition, we approximated the simulated actual residue r_{LHV} as the stoichiometric residue r_s and the interpolated residue r_s^{intrp} corresponding to the interpolated data curves in Fig. 4 was used for realistic simulation. In addition, the cycle-to-cycle variability of the stoichiometric residue was considered by adding residue variation of white noise process with the standard deviation shown in the error bars in Fig. 3 to r_s^{intrp}.

We compare the three schemes, SAFR, LHV and composite. For the cylinder flow estimator in Fig. 6, the estimator in [6] was used with the pumping map in the engine model [12] to estimate and correct MAF sensor biases.

The actual ethanol content change from 0 to 0.5 was simulated as shown in Fig. 10, and a throttle step was simulated from 34% to 38% at 140 sec as shown in Fig. 8. A 5% of MAF sensor bias and 5% of fuel injector shift were introduced to test the three methods. Fig. 9 shows

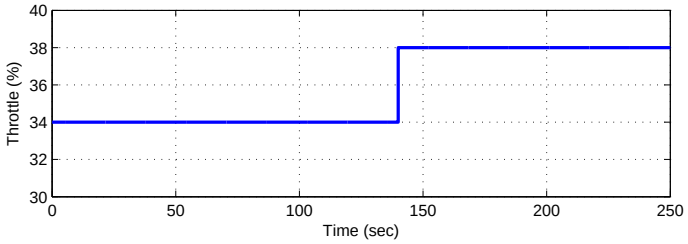

Figure 8: Simulated throttle input

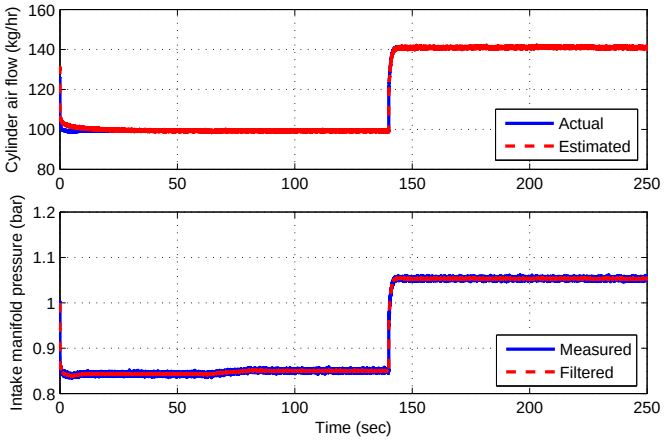

Figure 9: Simulated load for composite ethanol estimation

load conditions in composite ethanol estimation simulation. This plot indicates how successful is the cylinder air flow estimation when the MAF sensor bias estimation in [6] is applied.

Fig. 10 shows the fuel ethanol content estimation result. The SAFR-based estimation shows large steady state es-

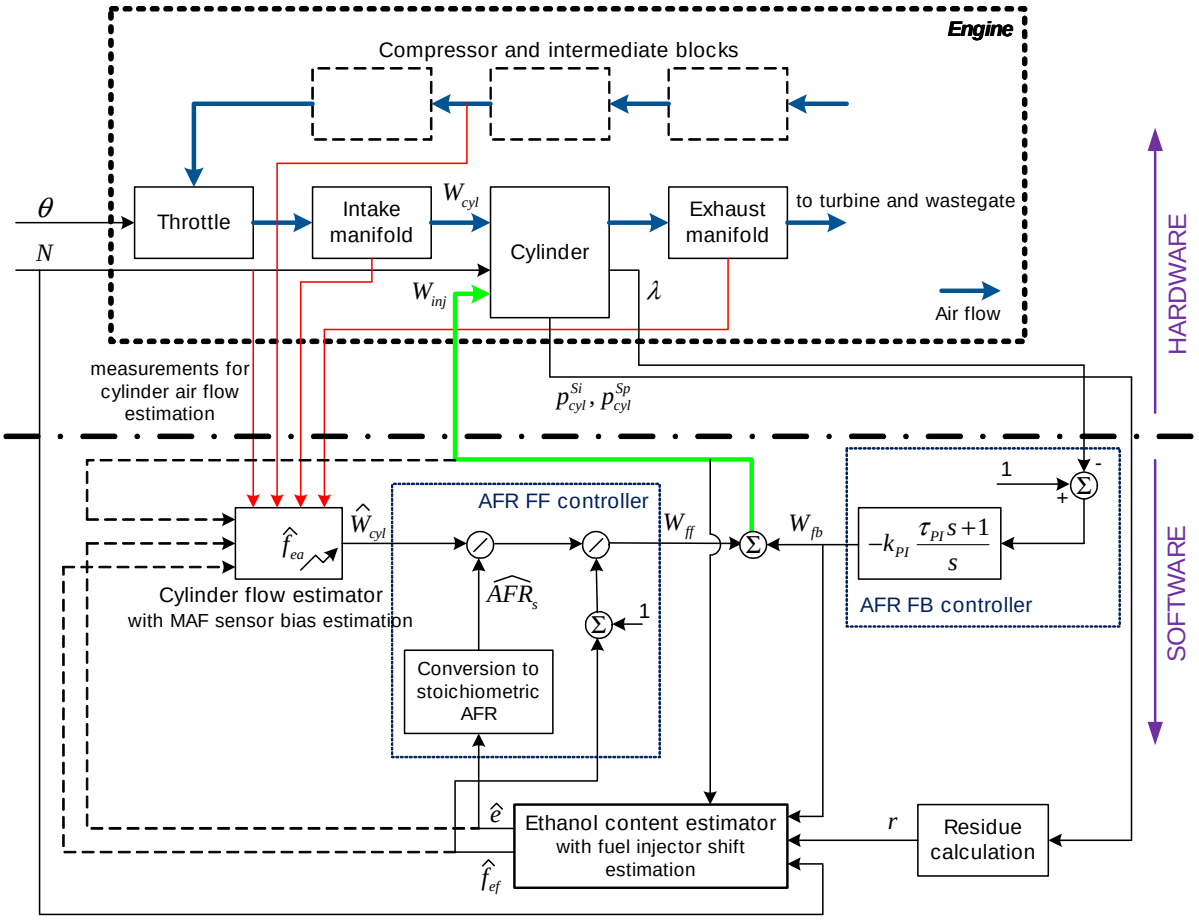

Figure 6: Block diagram of AFR control and composite ethanol estimation

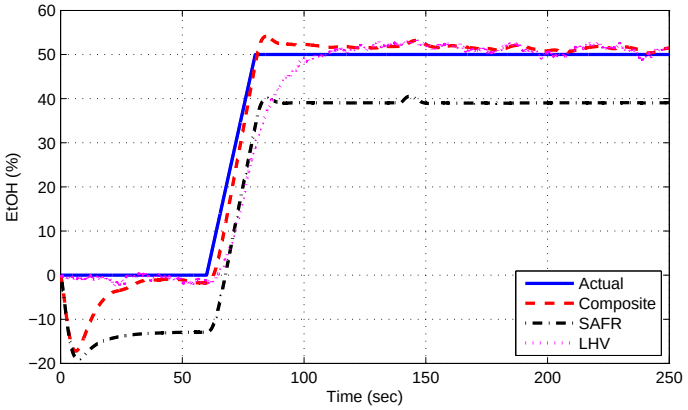

Figure 10: Simulated ethanol estimation

timation error due to the uncompensated fuel injector shift. The composite estimation shows improved steady state estimation performance by the virtue of simultaneous estimation hence compensation of the fuel injector shift. The LHV-based estimation shows small steady state estimation error as well, even though the response is noisy due to the cycle-to-cycle variability of detection residue. The steady state estimation performance for the LHV-based estimation is good because the steady state estimation is actually very insensitive to fuel injector shift at engine speed of 2500 RPM as shown in Fig. 5. On the other hand, convergence of the estimated ethanol content for LHV-based estimation is slower than that for composite estimation due to relatively low observer gain needed for filtering the residue cycle-to-cycle variability. The large cycle-to-cycle variability of detection residue is the main problem in realizing LHV-based estimation independent of the EGO sensor measurements. Fig. 11 shows the simu-

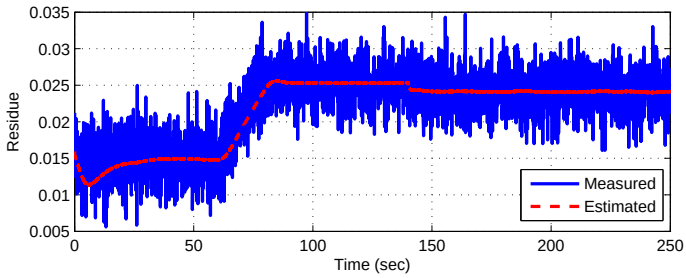

Figure 11: Simulated residue for composite ethanol estimation

lated residue for composite ethanol estimation. While the measured residue is very noisy due to the cycle-to-cycle variability of residue, the estimated stoichiometric residue, $\hat{r}_s$, is clean because estimated ethanol content, $\hat{e}$, is sufficiently clean and the modeled stoichiometric residue is relatively insensitive to the estimated fuel injection mass. The composite estimation exhibits good steady-state and fast convergence to the ethanol content. Fast convergence rate is important for overall vehicle performance enhancement as many other control and management algorithms in flex-fuel vehicles rely on the estimated ethanol

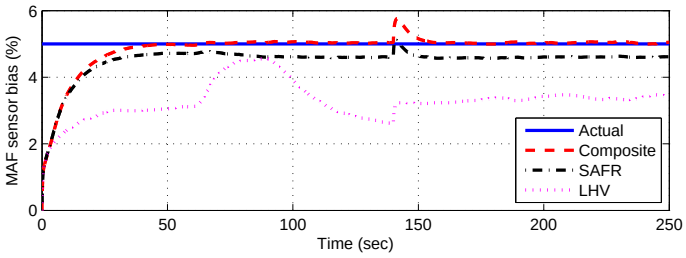

Figure 12: Simulated MAF sensor bias estimation

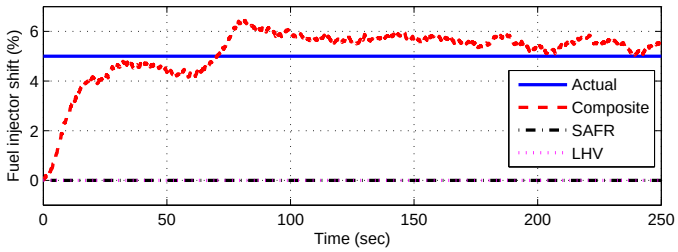

Figure 13: Simulated fuel injector shift estimation

content.

Fig. 12 and Fig. 13 show the MAF sensor bias estimation and the fuel injector shift estimation results, respectively. In the composite estimation, the fuel injector shift is estimated even though steady state error could not be completely removed due to the residue model uncertainty. In Fig. 12, the MAF sensor bias estimation is pretty good from the composite estimation, whereas the other schemes show more errors. This large error can be explained because the MAF sensor bias estimation scheme is actually coupled with the estimated fuel injection amount and the ethanol content. In Fig. 6, the dotted arrow lines into the cylinder flow estimator block indicate this dependency.

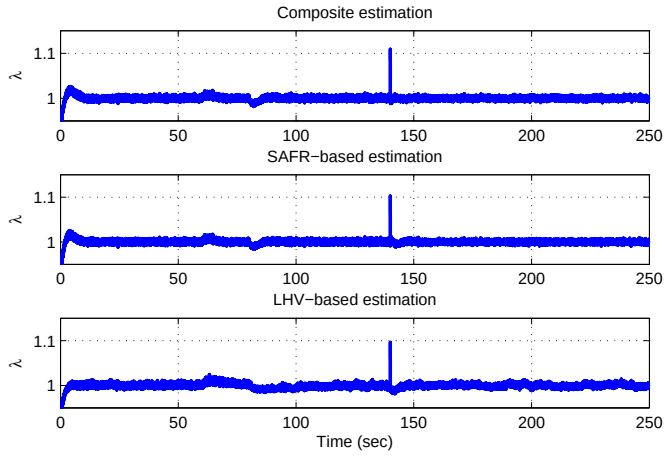

Figure 14: Simulated relative air-to-fuel ratio, λ

Fig. 14 shows simulated response of the relative AFR, λ. In all three estimation cases, λ is regulated near unity, while the response for the LHV-based estimation shows a little bit more fluctuations than those for others due to the noisier feedforward fuel command caused by noisier ethanol estimation originated from the cycle-to-cycle variability of detection residue. The spike at 140 sec corresponds to the throttle step change.

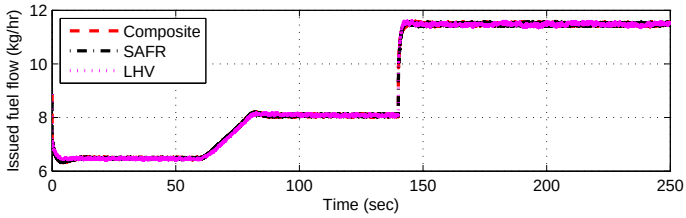

Figure 15: Simulated fuel injection command

Fig. 15 shows the issued fuel flow W_{inj} in the three estimation simulations. From 60 sec to 80 sec, fuel injection amount increases as fuel type is estimated to change from E0 to E50 since more ethanol content requires more fuel for stoichiometric combustion, and steep increase of fuel injection after 140 sec is observed due to the change of load.

8 CONCLUSION

In this paper, estimation of the ethanol content in flex fuel direct injection engines using the charge cooling or LHV-based detection residue calculated by in-cylinder pressure measurements together with EGO sensor measurements is proposed. Due to the high sensitivity of ethanol estimation error to MAF sensor bias and fuel injector shift in conventional SAFR-based estimation using the EGO sensor measurements, an estimation scheme that uses other sensor measurements to correct MAF sensor bias and fuel injector shift is required. Assuming MAF sensor bias could be estimated by using intake manifold pressure measurements,the simultaneous estimation of ethanol content and fuel injector shift using EGO and in-cylinder pressure measurements is shown.

High cycle-to-cycle variability of the LHV-based detection residue is observed. Due to this high cycle-to-cycle variability level in the cylinder pressure measurements, the estimator gain is chosen to realize sufficiently fast convergence to steady state in order to avoid noise amplification in estimated states. The ethanol detection residue retains high accuracy in limited operating conditions. In addition, stoichiometric residue shows a good property that it is relatively insensitive to fuel amount change. The validity and performance of the proposed composite ethanol estimator is verified by simulation with a flex-fuel SIDI engine model under MAF sensor bias and fuel injector shift.

APPENDIX: DETECTION SENSITIVITY

The applicability of a certain feature for fuel ethanol content estimation purpose depends on the high sensitivity of the feature to change of ethanol content. Therefore, several sensitivities need to be defined and investigated for the quantitative analysis of each feature we present in this paper. Let f_p denote a primitive feature. We assume that a primitive feature is primarily sensitive to ethanol content and insensitive to any other operating condition so that f_p is expressed by a function of e only, i.e., $f_p(e)$, where e

denotes the volumetric fraction of ethanol in the gasoline-ethanol fuel blend. Here, an ethanol *detection feature* is defined as a feature which is calculated by measurements from a specific sensor and also denoted by r. It is usually desirable that a detection feature is mainly affected by a specific primitive feature. A detection feature, r, might be then expressed as a function of a target primitive feature and engine operating conditions, i.e., $r(f_p(e), \boldsymbol{q})$, where $\boldsymbol{q}$ denotes a vector of engine operating condition variables. For example, λ is a detection feature which is calculated by the EGO sensor measurements that is associated with the primitive feature of stoichiometric AFR:

$$\lambda(AFR_s(e), m_a, m_f) = \frac{m_a}{m_f} \cdot \frac{1}{AFR_s(e)}, \qquad (18)$$

where m_a and m_f denote the fresh air charge mass and injected fuel mass per cycle. Here, the following two sensitivities are defined:

- *primitive feature sensitivity*: $S_{f_p} \triangleq \frac{1}{f_p} \cdot \frac{\partial f_p}{\partial e}$,
- *detection feature sensitivity*: $S_r \triangleq \frac{1}{r} \cdot \frac{\partial r}{\partial e} = \frac{f_p}{r} \cdot \frac{\partial r}{\partial f_p} S_{f_p}$.

High absolute value of detection feature sensitivity is desirable for ethanol estimation purpose, where detection feature sensitivity is very closely related to primitive feature sensitivity. For example, detection feature sensitivity for λ evaluated at stoichiometry is expressed by $S_\lambda\big|_s = -S_{AFR_s}$. If a detection feature can be expressed as a linear function of the associated primitive feature, i.e., $r = a(\boldsymbol{q}) f_p(e)$, the detection feature sensitivity is the same as the primitive feature sensitivity, $S_r = S_{f_p}$. If this is the case for heat of combustion (HC), i.e., if a detection feature associated with HC is a linear function of HC as well, the same level of detection feature sensitivity as that of λ at stoichiometry is expected, i.e., $\left|S_{r_{HC}}\right| \approx S_\lambda\big|_s$ since both primitive sensitivities are very similar, $S_{HC} \approx S_{AFR_s}$.

We still cannot conclude that two different ethanol estimation schemes based on different detection features are actually mutually independent even if the detection feature sensitivities are of the same magnitude. To quantify independency of different estimation schemes based on different detection features or independency of the detection features, one more sensitivity is defined: *relative detection sensitivity* of detection feature r with respect to an operating condition variable q is defined as

$$S_{r|q} \triangleq \frac{S_r}{\frac{\partial r/\partial q}{r/q}} = \frac{1}{q} \cdot \frac{\frac{\partial r}{\partial e}}{\frac{\partial r}{\partial q}}, \qquad (19)$$

where q is an element of operating condition vector $\boldsymbol{q}$. High absolute value of relative detection sensitivity is desirable for ethanol content estimation since frequently actual operating condition q is unavailable and estimation of q retains error and it is very common that limited knowledge about the functional structure of r in q is available. For example, relative detection sensitivity of λ with respect to injected fuel mass per cycle evaluated at stoichiometry is expressed by $S_{\lambda|m_f}\big|_s = S_{AFR_s}$. If a detection feature is expressed by a linear function in the associated primitive feature, i.e., $r = a(\boldsymbol{q}) f_p(e)$, the relative detection sensitivity of r with respect to q is expressed by $S_{r|q} = \frac{a/q}{\partial a/\partial q} S_{f_p}$.

Further, suppose that a detection feature associated with HC is expressed by multiple of total heat of combustion per cycle such that $r_{HC} = a(\boldsymbol{q}') \cdot m_f \cdot HC(e)$. The relative detection sensitivity of r_{HC} with respect to m_f is then $S_{r_{HC}|m_f} = S_{HC}$. In this case, we expect similar relative detection sensitivities for r_{HC} and λ at stoichiometry, $S_{r_{HC}|m_f} \approx S_{\lambda|m_f}\big|_s$, due to the similar primitive feature sensitivities, $S_{HC} \approx S_{AFR_s}$. If this is the case, we can conclude that SAFR-based estimation and HC-based estimation are not actually independent ethanol estimation schemes with respect to injected fuel mass. Both estimation schemes would then be prone to large ethanol estimation errors under fuel injector shift, or alternatively, the injector shift amount could not be estimated using both detection features.

We consider next the stoichiometric combustion with the indicated mean effective pressure (IMEP) calculated by the in-cylinder pressure measurements as the stoichiometric detection feature associated with HC. The mutual dependence of SAFR-based estimation and HC-based estimation becomes more clear after we consider the IMEP-based realization of the HC-based estimation. Stoichiometric IMEP at fixed other operating conditions than e and m_f or m_a is expressed by $imep_s = a \cdot m_f \cdot HC(e)$ with a constant a calibrated for the fixed operating conditions. Since $HC(e) \approx c \cdot AFR_s(e)$ where $c = 2.9$ MJ/kg, imposing the stoichiometry constraint $m_a/m_f = AFR_s(e)$ results in:

$$imep_s \approx ac \cdot m_a. \qquad (20)$$

Therefore calculating IMEP under closed loop stoichiometry control allows estimations of neither ethanol content e nor the fuel injector shift f_{ef}. The stoichiometric IMEP calculation is merely another version of mass air flow measurement.

REFERENCES

[1] Nakata, K., Utsumi, S., Ota, A., Kawatake, K., Kawai, T., and Tsunooka, T., "The effect of ethanol fuel on a spark ignition engine". *SAE paper 2006-01-3380*.

[2] Rocha, M. S., and Simões-Moreira, J. R. "A simple impedance method for determining ethanol and regular gasoline mixtures mass contents". *Fuel,* **84**, pp. 447–452, 2005.

[3] Wang, S. S., Lin, Y., Resendiz, N. H., Granados, L. E., and Rodriguez, H. H., "Ethanol concentration sensor". *SAE paper 2008-01-2452*.

[4] Ahn, K., Stefanopoulou, A. G., and Jankovic, M. "Estimation of ethanol content in flex-fuel vehicles using

an exhaust gas oxygen sensor: Model, tuning and sensitivity". In Proceedings of ASME 1st Annual Dynamic Systems and Control Conference, 2008.

[5] Theunissen, F., "Percent ethanol estimation on sensorless multi-fuel systems; advantages and limitations". *SAE paper 2003-01-3562*.

[6] Ahn, K., Stefanopoulou, A. G., and Jankovic, M. "Tolerant ethanol estimation in flex-fuel vehicles during MAF sensor drifts". In Proceedings of ASME 2nd Annual Dynamic Systems and Control Conference, 2009.

[7] Oliverio, N., Stefanopoulou, A., Jiang, L., and Yilmaz, H., "Ethanol detection in flex-fuel direct injection engines using in-cylinder pressure measurements". *SAE paper 2009-01-0657*.

[8] Oliverio, N. H., Jiang, L., Yilmaz, H., and Stefanopoulou, A. G. "Modeling the effect of fuel ethanol concentration on cylinder pressure evolution in direct-injection flex-fuel engines". In Proceedings of the 2009 American Control Conference, 2009.

[9] Furey, R. L., "Volatility characteristics of gasoline-alcohol and gasoline-ether fuel blends". *SAE paper 852116*.

[10] Furey, R. L., and Perry, K. L., "Vapor pressures of mixtures of gasolines and gasoline-alcohol blends". *SAE paper 861557*.

[11] Kar, K., Last, T., Haywood, C., and Raine, R., "Measurement of vapor pressures and enthalpies of vaporization of gasoline and ethanol blends and their effects on mixture preparation in an SI engines". *SAE paper 2008-01-0317*.

[12] Jiang, L., Vanier, J., Yilmaz, H., and Stefanopoulou, A., "Parameterization and simulation for a turbocharged spark ignition direct injection engine with variable valve timing". *SAE paper 2009-01-0680*.